

Macromolecular Materials and Engineering

Pore size distribution and blend composition affect in vitro pre-vascularized bone matrix formation on poly(vinyl alcohol)/gelatin sponges

--Manuscript Draft--

Manuscript Number:	mame.201700300R1
Full Title:	Pore size distribution and blend composition affect in vitro pre-vascularized bone matrix formation on poly(vinyl alcohol)/gelatin sponges
Article Type:	Communication
Section/Category:	
Keywords:	tissue engineering; scaffold; bioartificial; endothelial cells; Mesenchymal Stem Cells
Corresponding Author:	Serena Danti, Ph.D. University of Pisa Pisa, PI ITALY
Corresponding Author Secondary Information:	
Corresponding Author's Institution:	University of Pisa
Corresponding Author's Secondary Institution:	
First Author:	Jose Gustavo De la Ossa
First Author Secondary Information:	
Order of Authors:	Jose Gustavo De la Ossa Luisa Trombi Delfo D'Alessandro Lorenzo Pio Serino Maria Beatrice Coltelli Roberto Pini Andrea Lazzeri Mario Petrini Serena Danti, Ph.D.
Order of Authors Secondary Information:	
Abstract:	<p>This study was aimed at identifying compositional and architectural (pore size and distribution) parameters of biocompatible scaffolds, which could be best suitable for both osteoblasts and endothelial cells to produce optimized 3D co-cultured constructs. Spongy scaffolds were prepared using poly(vinyl alcohol) (PVA) and gelatin (G) at different weight compositions (PVA/G range: 100/0 - 50/50 w/w) via emulsion and freeze-drying. The higher gelatin content, the larger volume occupied by higher size pores. Human umbilical vein endothelial cells and human mesenchymal stromal cells were independently differentiated on the scaffolds to select the best candidate for the co-culture. The results of metabolic activity and histology on single platforms showed both cell- and material-type dependent outcomes. PVA/G 80/20 scaffolds were finally selected and allowed the formation of mineralized matrix containing organized endothelial-like structures. This study highlighted the need for systematic investigations on multifactorial parameters of scaffolds to improve vascularized bone substitutes.</p>
Additional Information:	
Question	Response
Please submit a plain text version of your	Dear Editor,

<p>cover letter here.</p> <p>Please note, if you are submitting a revision of your manuscript, there is an opportunity for you to provide your responses to the reviewers later; please do not add them to the cover letter.</p>	<p>It is my great pleasure to submit to Macromolecular Materials and Engineering on behalf of my co-authors, the revised version of our original manuscript entitled “Pore size distribution and blend composition affect in vitro pre-vascularized bone matrix formation on poly(vinyl alcohol)/gelatin sponges”</p> <p>by J.G. De la Ossa, L. Trombi, D. D’Alessandro, M.B. Coltelli, L.P. Serino, R. Pini, A. Lazzeri, M. Petrini, and S. Danti.</p> <p>Our research work relies on identifying compositional and architectural (pore size and distribution) parameters of biocompatible scaffolds, which could be best suitable for both osteoblasts and endothelial cells to produce optimal 3D co-cultured constructs via tissue engineering. Understanding the role played by physico-chemical and architectural parameters of porous scaffolds on both bone cells and endothelial cells can allow the development of in vitro pre-vascularized autologous bone substitutes, which may be functional and viable soon after implantation. Indeed, it has been shown that different cell types have different affinity towards specific scaffold features, including physico-chemical and architectural cues, and this undisclosed aspect can challenge the optimal scaffold choice. Little systematic work has been performed to reveal which scaffold parameters specifically affect cellular behaviors in co-cultured systems, in which bone and endothelial cells are ultimately required to synergize.</p> <p>Our study proposes a first systematic screening of some the parameters involved which may pave the way to understand and possibly predict such a complex cellular interplay. In particular, in this Communication we demonstrated that PVA/Gelatin 50/50 w/w, which accounted for the largest volume fraction of higher size pores, sustained endothelial, but osteoinduced-hMSC viability, thus suggesting that other parameters than pore size, as invoked by Karageorgiou and Kaplan (Biomaterials, 2005), possibly in combination, play key roles for achieving functional bone tissue engineering.</p> <p>I confirm that neither the manuscript nor any parts of its content are currently under consideration or published in another journal, but only as a conference abstract. Hoping that you may find our contribution innovative, interesting, and suitable for publication in Macromolecular Materials Engineering.</p> <p>We took into account the comments provided by the Reviewers.</p> <p>Yours sincerely, Serena Danti</p>
<p>Do you or any of your co-authors have a conflict of interest to declare?</p>	<p>No. The authors declare no conflict of interest.</p>

DOI: 10.1002/marc.((insert number)) ((or ppap., mabi., macp., mame., mren., mats.))

Communication

Pore size distribution and blend composition affect *in vitro* pre-vascularized bone matrix formation on poly(vinyl alcohol)/gelatin sponges^a

Dedicated to the memory of Prof. Michele Lisanti (1950-2017).

Jose Gustavo De la Ossa, Luisa Trombi, Delfo D'Alessandro, Maria Beatrice Coltelli, Lorenzo Pio Serino, Roberto Pini, Andrea Lazzeri, Mario Petrini, Serena Danti*

Mr. J.G. De la Ossa, Dr. D. D'Alessandro, Dr. L.P. Serino
OtoLab, Dept. of Surgical, Medical, Molecular Pathology & Emergency Medicine, University of Pisa, via Paradisa 2, 56124 Pisa, Italy.

jdelaossag@outlook.com

delfo.dalessandro@unipi.it

lorenzo.serino@inwind.it

Dr. L. Trombi, Prof. M. Petrini
Dept. of Clinical & Experimental Medicine, University of Pisa, via Savi 10, 56126 Pisa, Italy

l.trombi@yahoo.it

mario.petrini@med.unipi.it

Dr. M.B. Coltelli, Prof. A. Lazzeri, Dr. S. Danti
Dept. of Civil & Industrial Engineering, University of Pisa, Largo L. Lazzarino 2, 56122 Pisa, Italy.

mb.coltelli@ing.unipi.it

andrea.lazzeri@unipi.it

serena.danti@unipi.it

Dr. R. Pini
Institute of Ecosystem Study (ISE), National Research Council (CNR), via G. Moruzzi 1, 56124 Pisa, Italy

roberto.pini@ise.cnr.it

This study was aimed at identifying compositional and architectural (pore size and distribution) parameters of biocompatible scaffolds, which could be best suitable for both osteoblasts and endothelial cells to produce optimized 3D co-cultured constructs. Spongy scaffolds were prepared using poly(vinyl alcohol) (PVA) and gelatin (G) at different weight compositions (PVA/G range: 100/0 - 50/50 w/w) via emulsion and freeze-drying. The higher

^a **Supporting Information** is available online from the Wiley Online Library.

1
2
3
4
5
6
7
8
9
10
11
12
13
14
15
16
17
18
19
20
21
22
23
24
25
26
27
28
29
30
31
32
33
34
35
36
37
38
39
40
41
42
43
44
45
46
47
48
49
50
51
52
53
54
55
56
57
58
59
60
61
62
63
64
65

gelatin content, the larger volume occupied by higher size pores. Human umbilical vein endothelial cells and human mesenchymal stromal cells were independently differentiated on the scaffolds to select the best candidate for the co-culture. The results of metabolic activity and histology on single platforms showed both cell- and material-type dependent outcomes. PVA/G 80/20 scaffolds were finally selected and allowed the formation of mineralized matrix containing organized endothelial-like structures. This study highlighted the need for systematic investigations on multifactorial parameters of scaffolds to improve vascularized bone substitutes.

Key words: tissue engineering; scaffold; bioartificial; endothelial cells; mesenchymal stem cells

1. Introduction

1
2
3 Restoration of bone defects represent a widespread clinical problem occurring as a
4 consequence of several pathologies, such as trauma, tumor excision, chronic osteomyelitis,
5 non-union, avascular necrosis and spinal fusions.^[1] If the defect size is critical, bone
6 regeneration cannot occur spontaneously, leading to the necessity of surgical strategies that
7
8 avail themselves of bone substitutes; usually tissue grafts.^[2] Under innovative tissue
9
10 engineering approaches, autologous cells can be grown *in vitro* on biocompatible scaffolds
11 based on synthetic and/or biologic biomaterials and transplanted back to the patient, thus
12 reconstructing autologous bone with no need for tissue explants.^[3] Jeopardized failures of
13 bone tissue-engineered replacements have recently been reported to deal with unsuccessful
14 post-implant neo-vascularization.^[4] Indeed, the lack of an efficient vascular supply after
15 implantation may put at serious risk the survival of the transplanted cells. Therefore, the
16 development of non-surgical strategies able to promote microvasculature have become a
17 primary goal in bone tissue engineering.^[5,6,7] It has been pointed out that *in vivo* formation of
18 new blood vessels depended on the ordered interaction of endothelial cells with different cell
19 types, including mesenchymal stromal cells (MSCs).^[8,9,10] Among the various strategies
20 studied to foster the establishment of a functional vascular network in bone substitutes, co-
21 cultured systems, in which endothelial cells already coexist with bone cells at the time of
22 implantation, have been the subject of investigations in the last decade.^[5] Recent work has
23 focused upon setting up and studying three dimensional (3D) co-cultured systems to
24 comprehend the mechanisms underlying cell cross-talk with the ultimate purpose to empower
25 post-implant bone survival and integration.^[5] Independently of these studies, it has been
26 highlighted that bone cells, as well as other cell types, showed different affinity towards
27 diverse architectural cues of biomaterial scaffolds, pore size.^[11] However, little systematic
28 work has been performed to reveal which scaffold parameters specifically affect cellular
29
30
31
32
33
34
35
36
37
38
39
40
41
42
43
44
45
46
47
48
49
50
51
52
53
54
55
56
57
58
59
60
61
62
63
64
65

1 behaviors in co-cultured systems, in which bone and endothelial cells are ultimately required
2 to synergize.
3

4 This study was aimed at defining compositional and architectural features of biocompatible
5 spongy scaffolds which could be best suitable for both osteoblasts and endothelial cells, in
6 order to produce optimized 3D co-cultured constructs. Spongy scaffolds were prepared from
7 emulsions of a synthetic biocompatible polymer, poly(vinyl alcohol) (PVA), and a
8 biopolymer, gelatin (G), at different weight compositions (PVA/G range 100/0 - 50/50 w/w).
9 Human umbilical vein endothelial cells (HUVECs) and human MSCs (hMSCs) were
10 independently cultured and differentiated on all the sponge types to select the individual cell-
11 type affinity and to ultimately identify the best scaffold candidate for the co-culture.
12
13
14
15
16
17
18
19
20
21
22
23

24 Understanding the role played by physic-chemical and architectural parameters of porous
25 scaffolds on bone cells and endothelial cells can pave the way to developing *in vitro* pre-
26 vascularized autologous bone substitutes which may be functional and viable soon after
27 implantation.
28
29
30
31
32
33

34 35 36 37 **3. Results and Discussion** 38 39

40 Biomaterial-based substitutes for large bone defects offer the advantages of reproducibility
41 and biosafety, thus being promising alternatives to bone grafts under a tissue engineering
42 approach. Owing to the high costs necessary for a personalized therapy, it is important to
43 define the scaffold parameters that could best promote both formation and survival of bone
44 substitutes after surgery, the latter depending on the neo-vascularization of the implanted
45 cellular constructs.^[4] As a consequence, the selection of the optimal scaffold for bone
46 regeneration must take into account its capability of synergizing the interactions between
47 bone cells and endothelial cells. However, different cell types may show different affinity
48
49
50
51
52
53
54
55
56
57
58
59
60
61
62
63
64
65

1 towards specific scaffold features, including physico-chemical and architectural cues, and this
2 undisclosed aspect can challenge the optimal scaffold choice.^[11]
3

4 This study was aimed at investigating HUVEC and osteo-differentiated hMSC response
5 towards PVA/G sponges produced in a composition range in which G weight content was
6 increased from 0% up to 50%. Varying this parameter affected the scaffolds through physico-
7 chemical and architectural changes and ultimately resulted in different specifications by the
8 two cell types. An *ab initio* selection of those scaffold parameters can elucidate endothelial-
9 bone cell cross-talk mechanisms that would ultimately release best reliable *in vivo* implants
10 with increased success rate, which are key enabling factors in personalized therapy.
11
12
13
14
15
16
17
18
19
20
21

22 In tissue engineering, the scaffolds behave as engineered matrices that provide primary
23 structural support for 3D bone tissue formation by enabling bone extracellular matrix (ECM)
24 fundamental processes. PVA is a synthetic polymer, water soluble and nonhazardous, which
25 is used in several biomedical applications.^[12] It can be processed into several structures,
26 blended with proteins, and stabilized via physical and/or chemical crosslinking, thus acting as
27 a biostable material in the human body. Previous tissue engineering studies have focused only
28 on specific compositions of PVA/G hydrogels and sponges without any systematic
29 characterization.^[13,14,15,16,17]
30
31
32
33
34
35
36
37
38
39
40

41 The scaffolds produced in this study were analyzed using Fourier transmission infrared
42 (FTIR) spectroscopy to assess cross-linking and chemical effects of increasing G content in
43 the PVA/G blends.^[18] The general pattern of the PVA spectrum was in agreement with those
44 reported in literature (**Figure 1_A**).^[19] The higher G content, the stronger intensity of the 1635
45 cm^{-1} and 1535 cm^{-1} (amide I and amide II bands) typical of polyamides. By increasing G
46 content, only minor changes in the PVA band profile were observed, with the tendency of the
47 spectrum to increase in complexity showing several large bands in the range 1000-1500 cm^{-1} .^[20]
48 Cross-linking with glutaraldehyde (GTA) did not alter significantly the PVA infrared
49 spectrum. Differently, in presence of G, spectral changes were observed by comparing the
50
51
52
53
54
55
56
57
58
59
60
61
62
63
64
65

1 | uncross-linked with the cross-linked counterparts (**Figure 1 B, C**). For example, in cross-
2 | linked PVA/G 70/30 sample, a very weak shoulder at 1710 cm^{-1} appeared due to stretching
3 |
4 | C=O of GTA (**Figure 1 B**). Moreover, an increase in the band at 1130 cm^{-1} was present that
5 | has been attributed to C-O-C groups formation due to cross-linking reaction.^[21] In the PVA/G
6 |
7 | 50/50 sample, the shift from 1513 cm^{-1} to 1535 cm^{-1} of the G band was evident (**Figure 1 C**).
8 |
9 | This change reasonably occurred following linkage formation, as also observed in GTA cross-
10 |
11 | linked collagen samples.^[22] Moreover, in all the blends the double peak, typical of the
12 |
13 | uncross-linked PVA/G system at 1442 cm^{-1} and 1407 cm^{-1} caused by the overlapping of the
14 |
15 | bending CH_2 of PVA and G, became a unique peak centered at an intermediate wavelength
16 |
17 | for the cross-linked system. This is in agreement with the reaction of G with GTA,
18 |
19 | characterized by the presence of $-\text{CH}_2$, and thus leading to an alteration of the $-\text{CH}_2$ bending
20 |
21 | profile. Finally, the reaction of GTA with the $-\text{NH}_2$ groups of lysine residues allowed $\text{CH}=\text{N}$
22 |
23 | aldimine groups to be formed, with a characteristic absorption at 1450 cm^{-1} .^[18] Reasonably,
24 |
25 | the formation of this linkage is also responsible of the slight material yellowing after GTA
26 |
27 | cross-linking (**Figure 1**). FTIR analysis confirmed the compositional differences and the
28 |
29 | occurrence of cross-linking in all the samples ([Figure S1](#)).
30 |
31 |
32 |
33 |
34 |
35 |
36 |
37 |

38 | Porosity and pore interconnectivity are among the most important characteristics of a scaffold,
39 |
40 | because they greatly influence cell migration and molecule diffusion, finally facilitating the
41 |
42 | formation of bone ECM and vascularization processes. In general, large pore sizes can
43 |
44 | accommodate cell aggregates and ECM molecules, while small pore sizes play a role in
45 |
46 | fostering small molecule trafficking, such as nutrients, oxygen and catabolic products. In this
47 |
48 | view, the production of scaffolds containing several pore size classes is highly desirable to
49 |
50 | generate an optimal microenvironment for cell growth and differentiation. In particular, owing
51 |
52 | to large osteoblast size, migration requirements and transport phenomena, pores in the 100-
53 |
54 | $300\text{ }\mu\text{m}$ class and above are recommended to allow new bone ECM and capillary
55 |
56 | formation.^[23]
57 |
58 |
59 |
60 |
61 |
62 |
63 |
64 |
65 |

1 Under SEM, the inner structure of all the samples was found to consist of large pores of
2 spherical-like morphology provided with smaller intra-poral openings, thus providing proof of
3
4
5 interconnectivity (**Figure 2 A**). The porosimetric analysis ~~highlighted of~~ macropores ranging
6
7 in 0.08 – ~~300–125~~ μm , ~~with~~ ~~highlighted~~ a different distribution depending on PVA/G
8
9 composition (**Figure 2 B**). In particular, the volume filled by the 30 – 100 μm pore class
10
11 increased with increasing G content up to $83\% \pm 1\%$ in PVA/G 50/50, to the detriment of 10 –
12
13 30 μm and ~~0.08—10~~ μm classes. Conversely, the smaller 10—30 μm pore class was
14
15 predominant ($59\% \pm 10\%$) in PVA/G 100/0 (**Figure 2 B**). This finding can be attributed to the
16
17 foaming effect of G. After hydration in saline and culture media, PVA/G sponges were stable
18
19 over week-times.
20
21 The used crosslinking and post-treatment method prevented residual GTA-induced toxicity.
22
23 [13,14,15,16] PVA/G scaffolds were cultured *in vitro* to assess the scaffold interactions with
24
25 HUVECs and osteo-differentiated hMSCs, separately, ~~in order~~ to select the best candidate for
26
27 the co-culture. The results of metabolic activity indicated an enhanced viability of HUVECs
28
29 inside PVA/G 70/30 with respect to all the other compositions ($p < 0.05$), but 50/50 ($p = \text{n.s.}$)
30
31 (**Figure 3 A, B**). PVA/G 50/50 showed the second highest value that was not statistically
32
33 different from that detected in PVA/G 80/20 ($p = \text{n.s.}$). Differently, hMSCs cultured inside
34
35 PVA/G sponges displayed a statistically significant drop in metabolic activity along the
36
37 osteoinduction time in PVA/G 50/50 ($p < 0.05$). The best suitable PVA/G composition for
38
39 hMSCs was 80/20, followed by 70/30, the former being significantly increased with respect to
40
41 the initial time point ($p = 0.03$) and the highest at the endpoint among all ($p < 0.05$), but 70/30
42
43 ($p = \text{n.s.}$). Unlike in PVA/G 80/20, in 70/30 the hMSC viability at the endpoint did not
44
45 increase from the initial value ($p = \text{n.s.}$). An important aspect to take into account when *in*
46
47 *vitro* generating bone is the presence and morphology of the mineral matrix.^[24] A
48
49 morphologic analysis highlighted that well evident mineral nodules were found in PVA/G
50
51 80/20 and 70/30 (Figures 3 C and S2). Basing on the fact that good mineralization and
52
53
54
55
56
57
58
59
60
61
62
63
64
65

1 osteogenic cell viability are both fundamental aspects to create a functional bone substitute,
2 and that in our experimental plan HUVECs were to be seeded onto pre-generated bone
3 constructs, PVA/G 80/20 was finally chosen for the co-culture. However, PVA/G 70/30 was
4
5 to be considered a similarly suitable candidate. Interestingly, PVA/G 50/50 that accounted for
6
7 the largest volume fraction of high size pores did not sustain hMSC viability, thus suggesting
8
9 that other parameters than pore size affected bone formation. In fact, the results of metabolic
10
11 activity and histology on single cellular platforms clearly showed both cell- and material-type
12
13 dependent outcomes. It can be hypothesized that the combination of the polymeric blend
14
15 composition, its specific pore size distribution, and other topological and physical aspects,
16
17 altogether influenced each cell type with microenvironmental hints.
18
19

20
21
22
23 Finally, using PVA/G 80/20, after 23 osteoinduction days, viable MSC/scaffold constructs
24
25 were seeded with HUVECs and differentiated using Matrigel[®] to obtain endothelial tubes.
26
27 The results of the co-cultured constructs are shown in **Figure 4**. Cells ~~laden~~ ular rings onto the
28
29 pore surface and resembling tube-like structures could be frequently observed (**Figure 4 A,**
30
31 **C**). These cells were negative to von Kossa staining and positive to vascular endothelial
32
33 growth factor – 2 (VEGFR-2) immunostaining, which revealed endothelial cells. Differently,
34
35 osteoblasts were found located in large aggregates and embedded in mineral nodules (**Figure**
36
37 **4 A, C, D**). It has been reported that co-culture of endothelial cells with osteoblasts derived
38
39 from MSCs enhanced tube formation *in vitro* on 3D scaffolds due to the production of
40
41 cytokines and angiogenic growth factors, with scaffold composition and structure affecting
42
43 this cellular interplay.^[25,26] As an example, the addition of silk fibroin nanofibers to poly
44
45 (D,L-lactic acid) salt-leached scaffolds with similar porosity and pore size distribution, which
46
47 were otherwise highly suitable for co-culture, affected endothelial cell and osteoblast response
48
49 in a inhibitory way.^[26] The work of Stoppato and co-workers has nicely shown that either a
50
51 synergistic or depletive behavior of endothelial and bone cells can be observed depending on
52
53 certain scaffold architectural and compositional features. However, a systematic screening of
54
55
56
57
58
59
60
61
62
63
64
65

1 all the parameters involved is needed to understand and possibly predict such a complex
2 interplay.
3
4
5
6
7
8

9 **4. Conclusions**

10 FTIR analysis confirmed the compositional differences and the occurrence of cross-linking in
11 PVA/G sponges. The porosimetric analysis highlighted macropores ranging in 0.08—~~300~~
12 125 μm , with different distributions depending on PVA/G composition. Specifically, the
13 higher gelatin content, the larger volume occupied by higher size pores. The results of
14 metabolic activity and histology showed both cell- and material-type dependent outcomes.
15 PVA/G 80/20 scaffolds were finally selected for the co-culture and allowed the formation of
16 mineralized matrix containing organized endothelial-like structures. Interestingly, PVA/G
17 50/50, which accounted for the largest volume fraction of higher size pores, sustained
18 HUVEC, but osteoinduced-hMSC viability, thus suggesting that other parameters than pore
19 size play undisclosed roles for achieving functional bone tissue engineering.
20
21
22
23
24
25
26
27
28
29
30
31
32
33
34
35
36
37
38
39
40
41

42 **Supporting Information**

43 Supporting Information is available from the Wiley Online Library
44
45
46
47
48
49

50 Acknowledgements: The authors greatly acknowledge Dr. Sabrina Danti (University of Pisa)
51 for her technical contribute to statistical analysis and Prof. Stefano Berrettini (University of
52 Pisa) for hosting this research.
53
54
55
56
57
58
59

60 Received: Month XX, XXXX; Revised: Month XX, XXXX; Published online:
61
62
63
64
65

((For PPP, use “Accepted: Month XX, XXXX” instead of “Published online”)); DOI:

10.1002/marc.((insert number)) ((or ppap., mabi., macp., mame., mren., mats.))

1
2
3
4
5
6
7
8
9
10
11
12
13
14
15
16
17
18
19
20
21
22
23
24
25
26
27
28
29
30
31
32
33
34
35
36
37
38
39
40
41
42
43
44
45
46
47
48
49
50
51
52
53
54
55
56
57
58
59
60
61
62
63
64
65

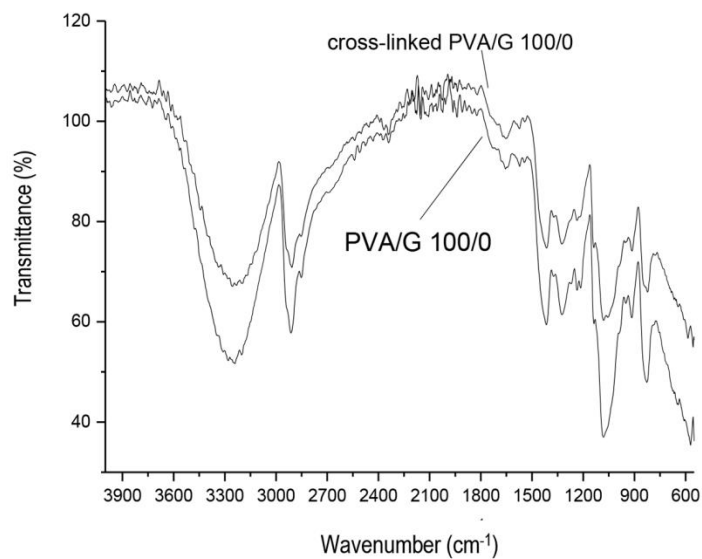
References

- 1
2 [1] M. J. Hubble, *Surg. Technol. Int.* **2002**, *10*, 261.
3
4 [2] Y. Fillingham, J. Jacobs, *Bone Joint J.* **2016**, *98-B*, (~~*1-Suppl A*~~) 6.
5
6 [3] J. Ng, K. Spiller, J. Bernhard, G. Vunjak-Novakovic, *Tissue Eng. Part B Rev.*, [DOI: doi.org/10.1089/ten.teb.2016.0289](https://doi.org/10.1089/ten.teb.2016.0289).
7
8
9
10
11 [4] M. I. Santos, R. L. Reis, *Macromol. Biosci.* **2010**, *10*, 12.
12
13 [5] Y. Liu, J. K. Chan, S. H. Teoh, *J. Tissue Eng. Regen. Med.* **2015**, *9*, 85.
14
15 [6] Á. E. Mercado-Pagán, A. M. Stahl, Y. Shanjani, Y. Yang, *Ann. Biomed. Eng.* **2015**, *43*,
16
17 718.
18
19 [7] L. H. Nguyen, N. Annabi, M. Nikkhah, H. Bae, L. Binan, S. Park, Y. Kang, Y. Yang, A.
20
21 Khademhosseini, *Tissue Eng. Part B Rev.* **2012**, *18*, [363](https://doi.org/10.1089/ten.teb.2012.0036).
22
23 [8] S. Almubarak, H. Nethercott, M. Freeberg, C. Beaudon, A. Jha, W. Jackson, R.
24
25 Marcucio, T. Miclau, K. Healy, C. Bahney, *Bone*. **2016**, *83*, [197](https://doi.org/10.1016/j.bone.2016.05.017).
26
27 [9] G. D. Barabaschi, V. Manoharan, Q. Li, L. E. Bertassoni, *Adv. Exp. Med. Biol.* **2015**, *881*,
28
29 [79](https://doi.org/10.1007/978-1-4939-9450-3_79).
30
31 [10] J. M. Kanczler, R. O. Oreffo, *Eur. Cell. Mater.* **2008**, *15*, [100](https://doi.org/10.1002/cm.2008.01100).
32
33 [11] P. Y. Huri, B. A. Ozilgen, D. L. Hutton, W. L. Grayson, *Biomed. Mater.* **2014**, *9*, [045003](https://doi.org/10.1088/1748-0227/9/4/045003).
34
35 [12] C. [M. Hassan](https://doi.org/10.1002/9781118471979.ch153), N. A. Peppas, [in Advance in Polymer -Science, Vol. 153, Springer, UK](https://doi.org/10.1002/9781118471979.ch153)
36
37 **2000**.
38
39 [13] M. G. Cascone, L. Lazzeri, E. Sparvoli, M. Scatena, L. P. Serino, S. Danti, *J. Mater. Sci.*
40
41 *Mater. Med.* **2004**, *15*, [121309](https://doi.org/10.1002/jbm.b.30139).
42
43 [14] S. Moscato, L. Mattii, D. D'Alessandro, M. G. Cascone, L. Lazzeri, L. P. Serino, A.
44
45 Dolfi, N. Bernardini, *Micron*. **2008**, *39*, [569](https://doi.org/10.1016/j.micron.2008.05.017).
46
47 [15] C. Ricci, C. Mota, S. Moscato, D. D'Alessandro, S. Ugel, S. Sartoris, V. Bronte, U.
48
49 Boggi, D. Campani, N. Funel, L. Moroni, S. Danti, *Biomatter* **2014**, *4*, [e955386](https://doi.org/10.1016/j.biomatter.2014.04.001).
50
51
52
53
54
55
56
57
58
59
60
61
62
63
64
65

- 1
2
3
4
5
6
7
8
9
10
11
12
13
14
15
16
17
18
19
20
21
22
23
24
25
26
27
28
29
30
31
32
33
34
35
36
37
38
39
40
41
42
43
44
45
46
47
48
49
50
51
52
53
54
55
56
57
58
59
60
61
62
63
64
65
- [16] S. Barachini, S. Danti, S. Pacini, D. D'Alessandro, V. Carnicelli, L. Trombi, S. Moscato, C. Mannari, S. Cei, M. Petrini, *Micron*. **2014**, *67*, [155](#).
- [17] S. Moscato, F. Ronca, D. Campani, S. Danti, *J. Funct. Biomater.* **2015**, *13*, [6](#), [16](#).
- [18] T. H. Nguyen, B.T. Lee, *J. Biomed. Sci. Eng.* **2010**, *3*, [1117](#).
- [19] G. M. Kim, [Fabrication of Bio-nanocomposite Nanofibers Mimicking the Mineralized Hard Tissues via Electrospinning Process](#), in *Nanofibers*, (Ed. A. Kumar), InTech, [Croatia 2010](#), [Ch. 4](#).
- [20] M. Bertoldo, M. B. Coltelli, T. Messina, S. Bronco, V. Castelvetro, *ACS Biomater. Sci. Eng.* **2016**, *2*, [677](#).
- [21] G. A. Ari, Z. Özcan, *Synthetic Metals*. **2016**, *220*, [269](#).
- [22] M. C. Chang, J. Tanaka, *Biomaterials*. **2002**, *23*, 4811.
- [23] V. Karageorgiou, D. Kaplan, *Biomaterials*. **2005**, *26*, [5474](#).
- [24] E. Parker, A. Shiga, J. E. Davies, [Growing Human Bone In Vitro](#) In *Bone Engineering*, (Ed. JE Davies), EM Squared Inc., Toronto, Canada **2000**, p. 63.
- [25] K. Wang, L. Cai, F. Hao, X. Xu, M. Cui, S. Wang, *Biomacromolecules*. **2010**, *11*, [10](#) 2748.
- [26] M. Stoppato, H. Y. Stevens, E. Carletti, C. Migliaresi, A. Motta, R. E. Guldberg, *Acta Biomater.* **2015**, *25*, [16](#).

Figures

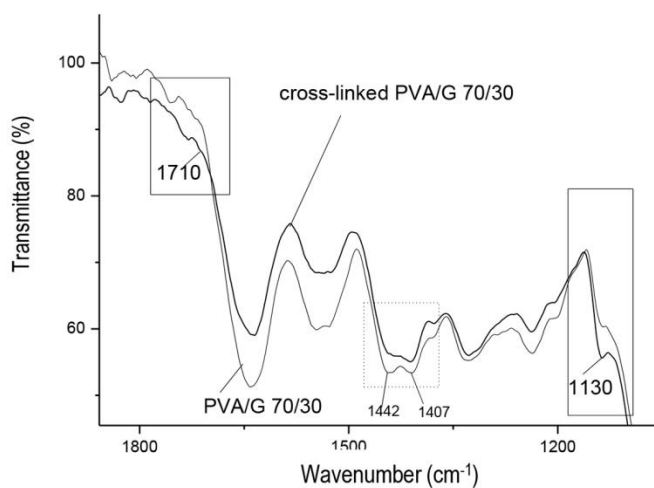
A



**PVA/G 100/0
Cross-linked**



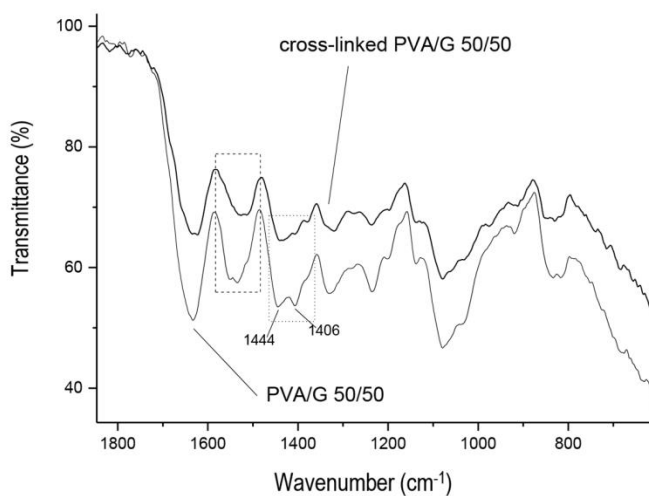
B



**PVA/G 70/30
Cross-linked**



C



**PVA/G 50/50
Cross-linked**



Figure 1. Representative FTIR spectra (cross-linked and uncross-linked) and respective pictures of: (A) PVA/G 100/0, (B) PVA/G 70/30, and (C) PVA/G 50/50 w/w.

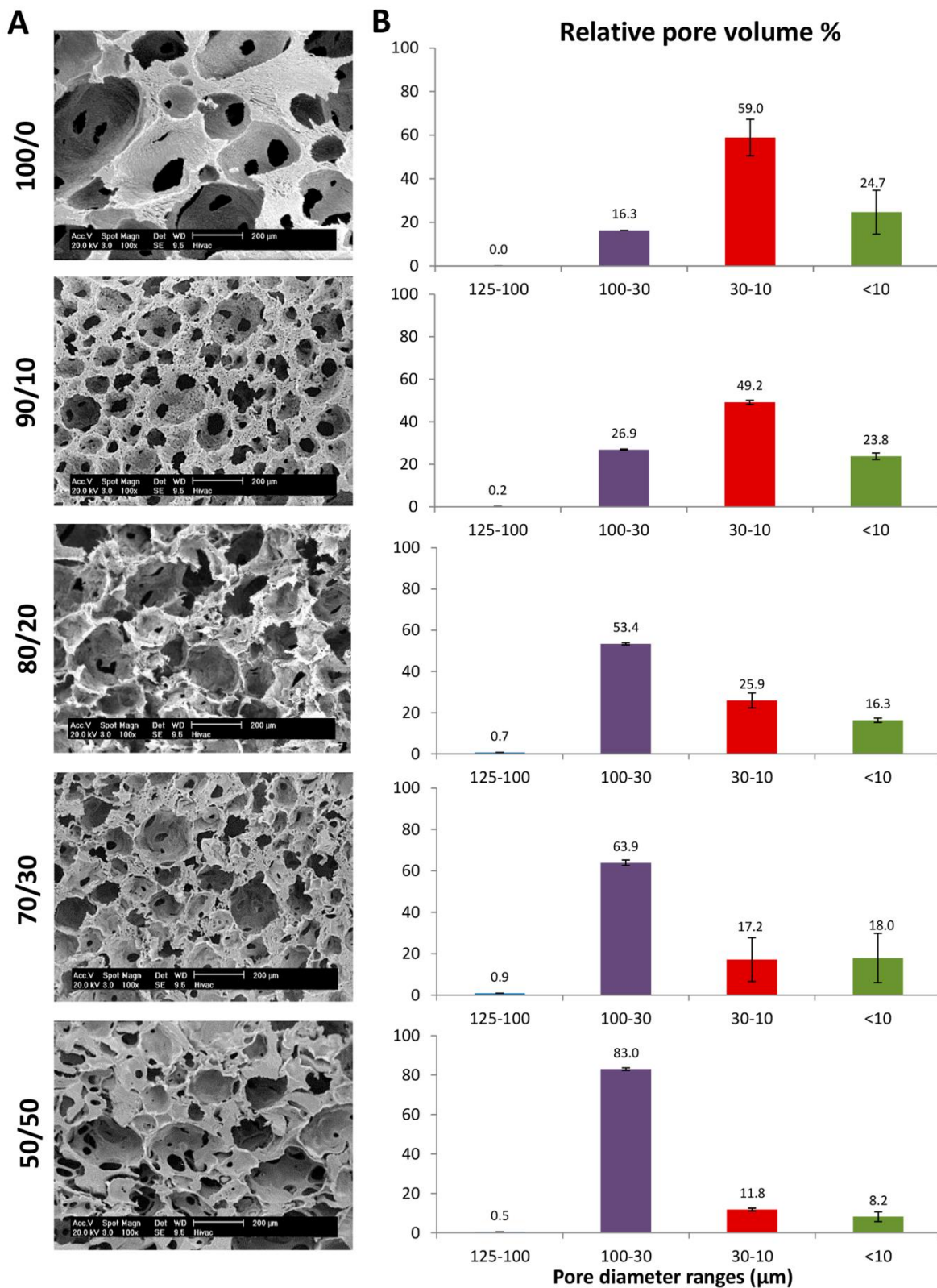


Figure 2. Results of SEM (A) and mercury intrusion porosimetry (B) for all the produced sponges showing pore morphology and pore size distribution, respectively.

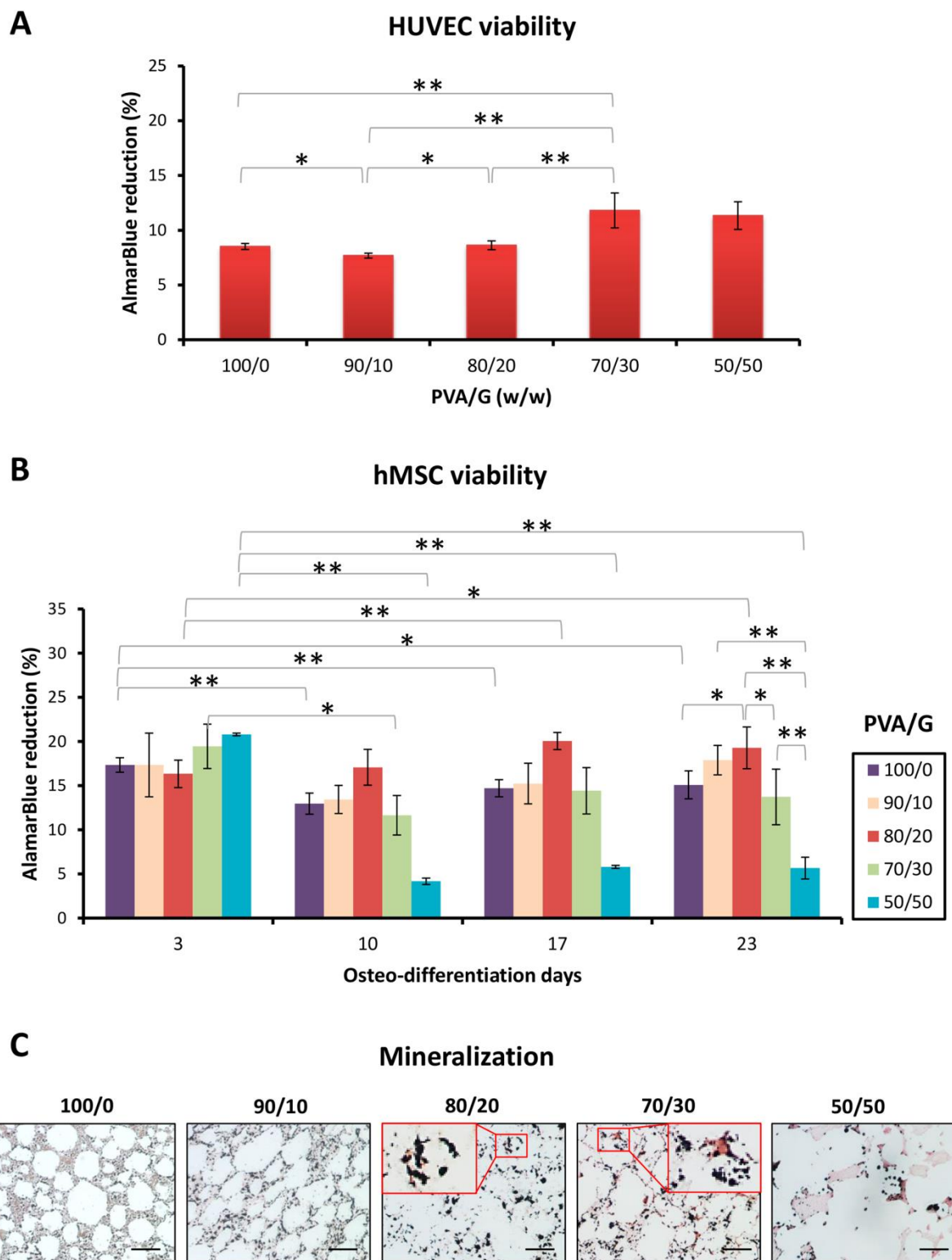


Figure 3. Biological results: cell viability (A,B) and von Kossa staining (C) for HUVECs (A) and osteoinduced hMSCs (B,C) in all the produced scaffolds. (C) Calcium deposits are stained in black; scale bar is 100 μ m.

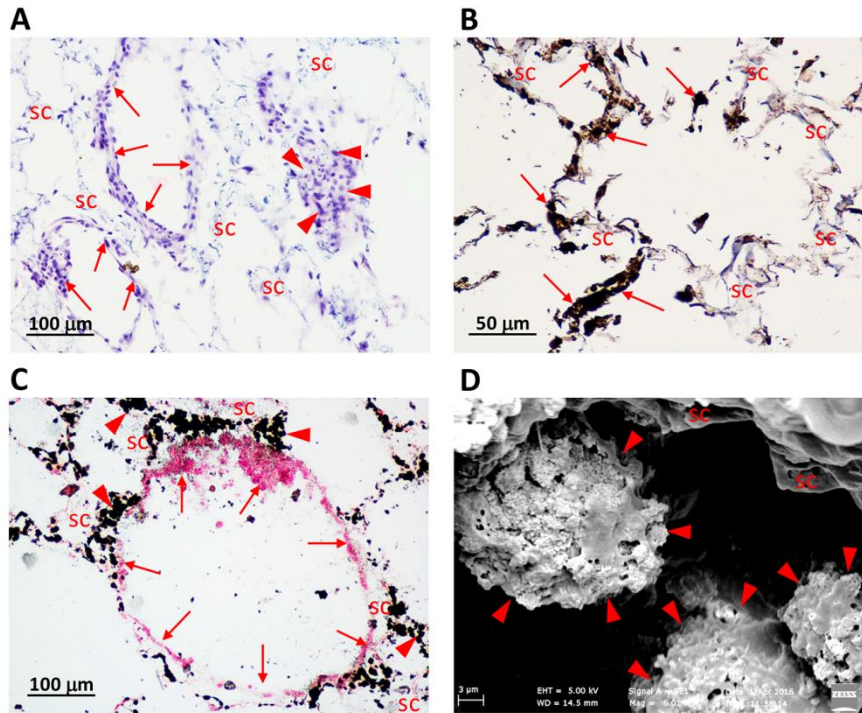


Figure 4. Results of the co-cultured construct: PVA/G 80/20 scaffold cultured with osteoinduced hMSCs and HUVECs: (A) H&E staining showing cell nuclei in blue and cytoplasm in pink; (B) VEGF-2 immunoreaction in dark brown showing endothelial cells; (C) von Kossa staining showing calcium deposits in black and cells in red; and (D) SEM analysis showing osteoblast-like cells and mineral-like matrix deposition. Arrows point to endothelial cells, while arrowheads to osteoblasts, “sc” is scaffold material.

Word count: 2997

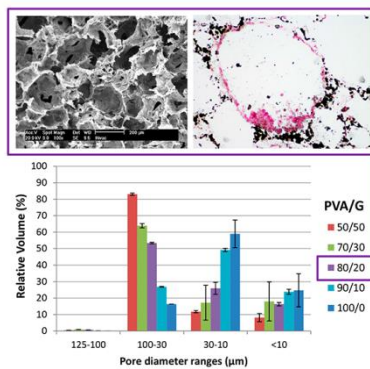
Table of contents

PVA/gelatin scaffolds were produced via emulsion and freeze-drying from 100/0 to 50/50 w/w compositions. Changing composition affected pore size distribution and biological response of endothelial cells and mesenchymal stromal cells, including metabolic activity and differentiation. PVA/gelatin 80/20 scaffolds allowed the formation of mineralized matrix containing organized endothelial-like structures. Systematic investigations on physico-chemical and architectural features can improve vascularized bone substitutes.

De la Ossa J.G., Trombi L., D'Alessandro D., Coltelli M.B., Serino L.P., Pini R., Lazzeri A., Mario P., Danti S.*

Pore size distribution and blend composition affect *in vitro* pre-vascularized bone matrix formation on poly(vinyl alcohol)/gelatin sponges

ToC figure



1
2
3
4
5
6
7
8
9
10
11
12
13
14
15
16
17
18
19
20
21
22
23
24
25
26
27
28
29
30
31
32
33
34
35
36
37
38
39
40
41
42
43
44
45
46
47
48
49
50
51
52
53
54
55
56
57
58
59
60
61
62
63
64
65



Click here to access/download
Supporting Information
Supplementary for revision.docx

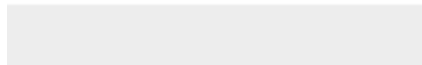
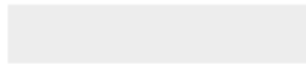




Click here to access/download

Production Data


Danti_manuscript MSE_R1.docx







Click here to access/download
Production Data
Figure-1.tif



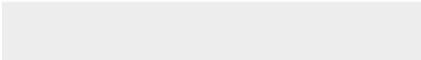




Click here to access/download
Production Data
Figure-2.tif






Click here to access/download
Production Data
Figure-3.tif





Click here to access/download
Production Data
Figure-4.tif





Click here to access/download
Production Data
Supplementary.docx





Click here to access/download
Production Data
ToC Figure.tif

